Journal of Experimental Nanoscience
Publication details, including instructions for authors and subscription information:
http://www.informaworld.com/smpp/title~content=t716100757

Optical emission and absorption spectra of Zn-ZnO core-shell nanostructures

Avijit Ghosh[a]; R. N. P. Choudhary[a]
[a] Department of Physics & Meteorology, Indian Institute of Technology Kharagpur, Kharagpur 721302, India

Online publication date: 24 March 2010

To cite this Article Ghosh, Avijit and Choudhary, R. N. P.(2010) 'Optical emission and absorption spectra of Zn-ZnO core-shell nanostructures', Journal of Experimental Nanoscience, 5: 2, 134 — 142
To link to this Article: DOI: 10.1080/17458080903321829
URL: http://dx.doi.org/10.1080/17458080903321829

Journal of Experimental Nanoscience
Vol. 5, No. 2, April 2010, 134–142

Taylor & Francis
Taylor & Francis Group

Optical emission and absorption spectra of Zn–ZnO core-shell nanostructures

Avijit Ghosh and R.N.P. Choudhary*

Department of Physics & Meteorology, Indian Institute of Technology Kharagpur, Kharagpur 721302, India

(*Received 17 March 2009; final version received 7 September 2009*)

The core-shell Zn–ZnO nanostructures were fabricated from Zn-powder embedded in graphite (i.e. carbon matrix) in a thin-films form by an inexpensive vacuum arc technique followed by laser ablation. The grazing incidence X-ray diffraction pattern shows that intensity of Zn-peak decreases, and subtle ZnO-peak increasing with the increase in laser power. The high resolution transmission electron microscopic study clearly exhibits the formation of a core-shell nanostructure as fabricated by laser ablation. The emission characteristics of laser ablated (with different powers) samples show a strong exciton peak at 388 nm, and a few more weak peaks (due to weak defect states in the visible range). The optical absorption spectra were obtained from the excitonic peaks (from 344 nm to 317 nm) on decreasing laser power. These peaks occur due to the coupling of exciton absorption (from ZnO shell layer) and core metal interband absorption. The Zn–ZnO core-shell nanostructure is useful for nanophotonic applications.

Keywords: core-shell structure; photoluminescence; UV absorption

1. Introduction

Nowadays, the motivation of current research activity in the field of nanotechnology is to tune physical properties of the nanostructures by controlling their shape and size. Some self-assembled metal and/or semiconductor composite nanomaterials are promising candidates for the fabrication of future nanodevices. This is due to microstructures (epitaxial relationship, misfit relaxation, etc.) of the interconnect materials at nanoscale. The formation of core-shell nanostructure of metal with self-assembled oxide layers enables us to manipulate the physical properties (i.e. electronic, optical, magnetic, biomedical) of the surface for required applications. In the present study, we have attempted to fabricate such core-shell Zn–ZnO nanostructures, and studied their emission and absorption properties. This type of unique facet-controlled nanostructures improves the electron transport properties since the metal core acts as a current-collecting electrode inside to maintain the large surface area. Because of the difficulties in formation of

*Corresponding author. Email: crnpfl@phy.iitkgp.ernet.in

ISSN 1745–8080 print/ISSN 1745–8099 online

DOI: 10.1080/17458080903321829
http://www.informaworld.com

required core-shell structures of Zn–ZnO, (comprising a metal core and an oxide shell), only a few attempts have been made in the past. Some of the methods reported in the literatures are vapour–liquid–solid (VLS) [1], Zn/F sequential ion implantation [2], laser ablation in liquid media [3], thermal reduction [4] and eletrodeposition [5]. Unfortunately, these methods are expensive and require rigorous experimental conditions. Therefore, it is essential to develop a cost effective fabrication technique for large scale production. Rapid laser ablation method is one such cost effective technique that has been successfully adopted in our laboratory to fabricate core-shell Zn–ZnO nanostructures. As reported earlier, the photoluminescence (PL) spectra of ZnO exhibit emission bands in ultra-violet (UV) [6] and visible (green [7], blue [8] and violet [9]) regions. The UV-peak is considered to be the characteristic emission of ZnO, and is attributed to the band edge emission or the exciton transition. The emission in the visible region is associated with the intrinsic defects of ZnO, even though there exists a lot of controversies in the dominant intrinsic defects [10–12]. From the detailed studies of UV absorption mechanism, it has been shown that blue shift of absorbance shoulder may be due to exciton absorption of ZnO [13,14]. However, there is still an open question for the physical basis of absorption peak of Zn–ZnO nanostructure at lower wavelength.

Therefore, in order to get a better understanding of the characteristic PL emission with intrinsic defects and UV-Visible absorption mechanism in Zn–ZnO core-shell nanostructure, we have carried out this work. In this article, we report the fabrication of the Zn–ZnO nanostructures by laser ablation (in thin-films form) followed by their detailed studies of UV-Visible emission and absorption characteristics.

2. Experimental

For the fabrication of the Zn–ZnO nanostructures, thin film of carbon encapsulated Zn nanoparticles on glass substrates was prepared using a modified Huffman–Krätschmer carbon arc method [15] in vacuum (10^{-3} Torr) using high purity (99.5%) Zn dust (M/S LOBA Chemicals) and aqueous conductive graphite (99.9%, M/S Alfa Aesar). The film was then laser ablated by a line tunable transverse excited atmospheric (TEA) pressure CO_2 laser. The power of CO_2 laser was optimised by controlling voltage and ratio of $CO_2 : N_2 : He$ was $1 : 2 : 4$. The gas pressure (800 mbar) was optimised to get emission pulses at 9.22 μm wavelength with the pulse energy of 1.5 J over a temporal duration of ~3 μs. The power supply of the laser source charged the high voltage main capacitors in laser head to a voltage up to several kilovolts. The laser ablation was carried out at 24 kV, 26 kV and 28 kV with a resonating frequency of 30 kHz.

Structural characterisation of the samples was carried out by a grazing incidence X-ray diffraction (GIXRD) technique using a PHILLIPS XPERT-PRO diffractometer with CuK_α radiation ($\lambda = 0.154$ nm) in an angle of incidence of 1° over an angular range of $30° \leq 2\theta \leq 60°$ with a step size of 0.02°. The transmission electron micrograph of the laser ablated samples was recorded using a high resolution transmission electron microscope (HRTEM) with JEOL JEM-2100F with an accelerating voltage of 200 kV. The surface morphology of Zn–ZnO nanostructure was recorded by field emission scanning electron microscopy (FESEM ZEISS).

Room temperature PL spectra were recorded using a PERKIN ELMER LS-55 spectrometer with a xenon lamp at the excitation wavelength of 325 nm.

Room temperature absorption spectra of these samples were obtained using a PERKIN ELMER Lambda 45 UV-VIS spectrophotometer.

3. Results and discussion

Figure 1(a)–(c) shows the GIXRD pattern of the laser ablated samples with different powers of the TEA-CO_2 laser. The diffraction peaks of metallic zinc are observed in all the samples with small peaks of hexagonal zinc oxide. All the diffraction peaks for Zn and ZnO are indexed. The coexistence of Zn and ZnO is evident from the diffraction pattern. It is noticed that on lowering the laser power, the intensity of ZnO peak (i.e. nearly nanocrystalline to amorphous phase) is reduced significantly. This is because of the energy released from the lowered laser power is not high enough for ordering of ZnO in crystalline form.

Figure 2 shows a typical TEM image of a Zn–ZnO nanocluster (laser ablation was carried out at 26 kV) sample. The existence of some Zn–ZnO nanoclusters in the sample is observed in Figure 2(a) (inset). The selected area electron diffraction (SAED) pattern of the corresponding nanocluster (Figure 2b) exhibits the prominent Zn pattern only. The size distribution of the Zn–ZnO nanostructure is shown in Figure 3. From the Figure, it is clear that there is non-uniform distribution of nanoparticles. The size distribution obtained from the TEM was fitted to a Gaussian function, as shown in Figure 3, and the estimated average size was 13.18 nm. The morphology of high-magnification TEM exhibits metallic Zn nanoparticles in core with a diameter of 12 nm embedded in ZnO shell of diameter around 2.5 nm. This, in turn, indicates that on increasing the laser power, the shell thickness increases. When the high power laser pulse is incident on the carbon

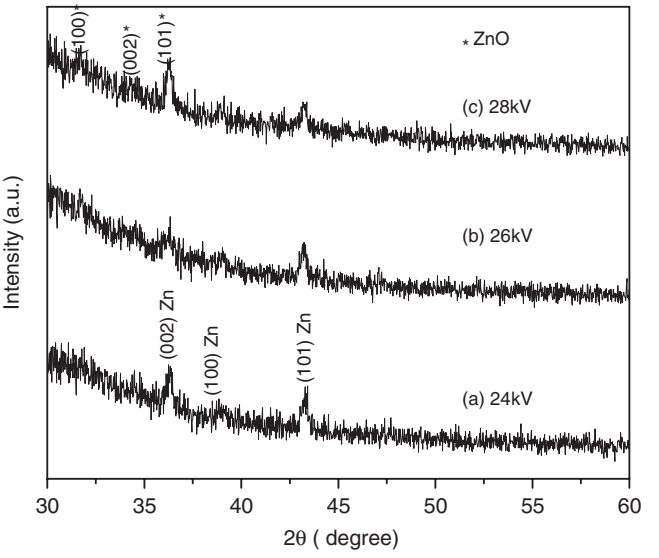

Figure 1. GIXRD pattern of laser ablated Zn–ZnO thin film at different laser power (24 kV, 26 kV, 28 kV).

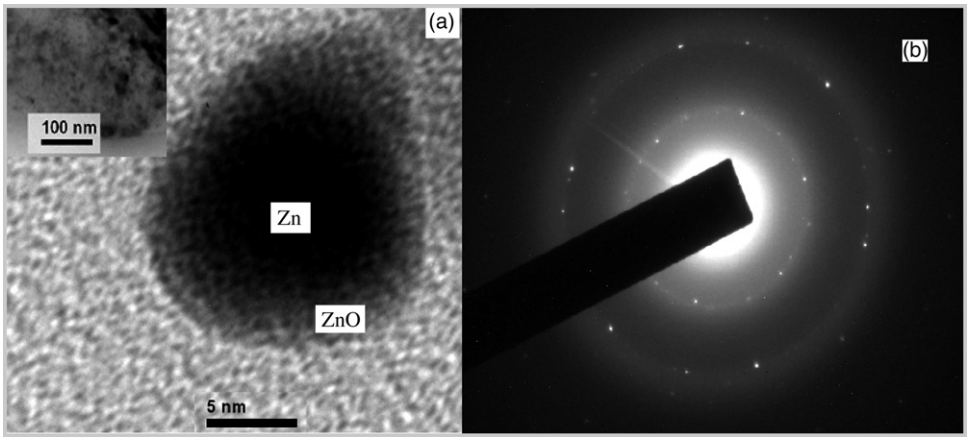

Figure 2. (a) High resolution TEM image of core-shell Zn–ZnO nanostructure and TEM image of Zn–ZnO nanostructure (inset) and (b) SAED pattern for Zn–ZnO nanostructure (laser ablation was carried out at 26 kV).

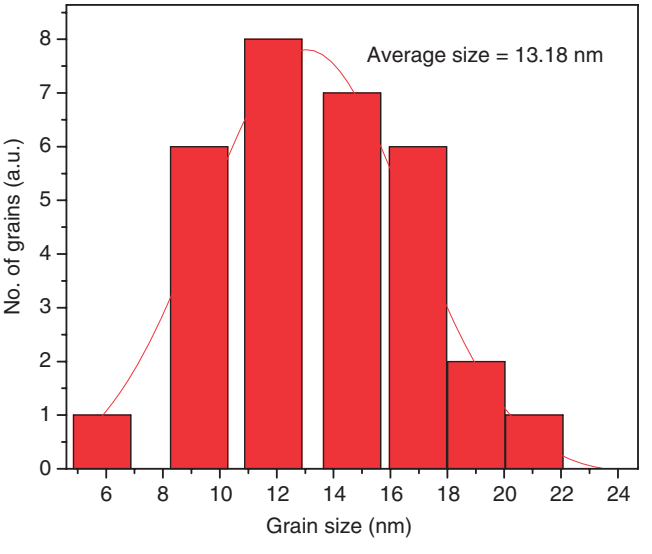

Figure 3. The size distribution obtained from Gaussian fit to the TEM histogram of the Zn–ZnO nanostructured film (laser ablation was carried out at 26 kV).

encapsulated zinc nanoparticles, the carbon matrix is burnt, and the high impact melts the Zn particles. Since the incident pulse is of very short duration, only an outside thin layer is oxidised. As a result, the existence of Zn inside the ZnO shell layer is observed. The FESEM image (Figure 4) clearly suggests that aggregation of nanocrystallites occurs due to high power pulsed laser irradiation.

Room temperature optical properties of the fabricated core-shell nanostructures were analysed using a PL technique. Figure 5(a) shows the PL spectra of the core-shell Zn–ZnO

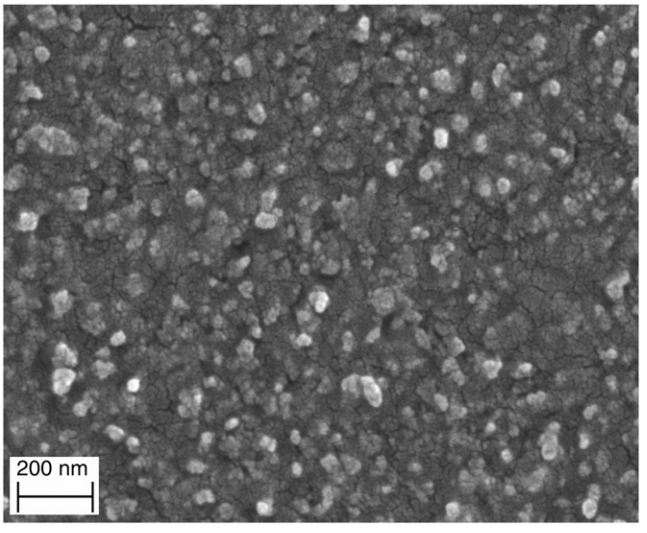

Figure 4. Typical FESEM image of Zn–ZnO nanostructured thin film ((laser ablation was carried out at 26 kV).

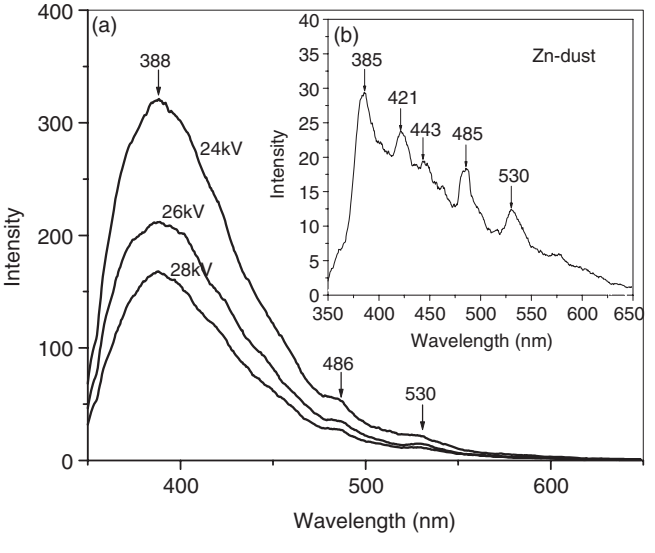

Figure 5. (a) Room temperature PL spectra of Zn–ZnO nanostructured thin film at different laser power and (b) PL spectra of Zn-dust (inset).

nanostructures ablated at different laser power. On lowering the laser power, Zn–ZnO core-shell structure creates more optically active point defect states due to the presence of Zn inside ZnO shell. All the samples exhibit a prominent UV emission peak at 388 nm with long tail in a deep level region with two distinct optically active defect states: very weak blue (486 nm) and green (530 nm) emission peaks. However, we did not get any signature of violet emission as reported [5,13] earlier in the Zn–ZnO core-shell structure. The UV

emission peak with long tail (in the deep level region) increases on lowering the laser power, whereas peak position remains unchanged. In addition, the full width at half maxima (FWHM) of PL peak increases on lowering the laser power. The high value of UV to visible emission peak ratio suggests the formation of high quality of core-shell nanostructure (i.e. less defect states at the surface). The inhomogeneity in broadening of the PL spectrum of Zn–ZnO nanostructure arises due to surface defects, impurity, particle size fluctuation, etc. The core-shell structures fabricated by the laser ablated method have some defects at the Zn and ZnO interface of core-shell structures. The PL spectra do not show any quantum confinement effect, although with thickness of ZnO shell layer of diameter around 2.5 nm. It may be due to large size distribution of the Zn–ZnO system. This assumption can be confirmed by broad absorption edge. Room temperature PL peak observed at 388 nm may be due to large exciton binding energy (i.e. 60 meV of ZnO). Again, due to thermal energy (at room temperature) bound excitons (due to small binding energy, few millielectronvolts) may be divided into free excitons. The laser ablated Zn–ZnO nanostructures show the red shifting at 3.2 eV as compared to the reported free exciton peak position at 3.26 eV [16]. Depending on transformation of ZnO nanocrystalline to form amorphous phase in Zn–ZnO core-shell structure, recombination of excitons may take place through exciton–exciton collision process even at room temperature. As a result, one of the excitons recombines radiatively to generate a photon [17], which results in increasing in PL intensity monotonically. The intensity of PL spectrum (Figure 5b) of Zn dust (due to surface oxidation) differs from that of Zn–ZnO core-shell nanostructure. The strong UV emission of Zn-dust is the same as ZnO bulk (peak centred at 385 nm). The other strong defect-related emissions of Zn-dust were found centred at 421, 443, 485 and 530 nm. As the structure and point defects are the origin of non-radiative recombination centres, they are responsible for deep level emission. Therefore, the low point defect concentration in material is essential to increase the internal quantum efficiency of the near-band-edge emission. Using full-potential linear muffin-tin orbital method [18–21], energy level of various defect centres (i.e. vacancies of oxygen and zinc, antisite oxygen, interstitial zinc and oxygen) of ZnO film was calculated. It is found that the energy gap between zinc interstitial (Zn_i) level to that of zinc vacancy (V_{Zn}) is 2.6 eV, which is comparable to 2.55 eV (for blue emission). Therefore, deep level blue emission is responsible for the electronic transition from energy level of zinc interstitial (Zn_i) to that of zinc vacancy (V_{Zn}). The green emission observed at 530 nm in the PL spectrum is attributed to the radiative transition of electrons from the conduction band to the local defect energy level of oxygen antisite (O_{Zn}) rather than the oxygen interstitial (O_i) defect energy level in Zn–ZnO nanostructure. The probability of forming O_i is very small due to a large diameter of oxygen atom [20].

The optical absorption spectra obtained at room temperature are shown in Figure 6. It is interesting to note that the intensity of absorption spectrum drastically reduces at short wavelength on lowering laser power. The prominent exciton absorption peak shifts from 344 nm (3.6 eV) to 317 nm (3.9 eV) in the UV range of Zn–ZnO nanostructure. The change in the excitonic structure of Zn–ZnO (due to local heating effect of laser power) analyses the optical quality of core-shell nanostructure. The presence of metallic Zn in the structure is evident from the GIXRD diffraction pattern. There is no signature corresponding to absorption peak due to surface plasmon resonance effect [22,23] for Zn metal nanoparticles (due to coulombic interaction by dielectric screening). Usually, excess

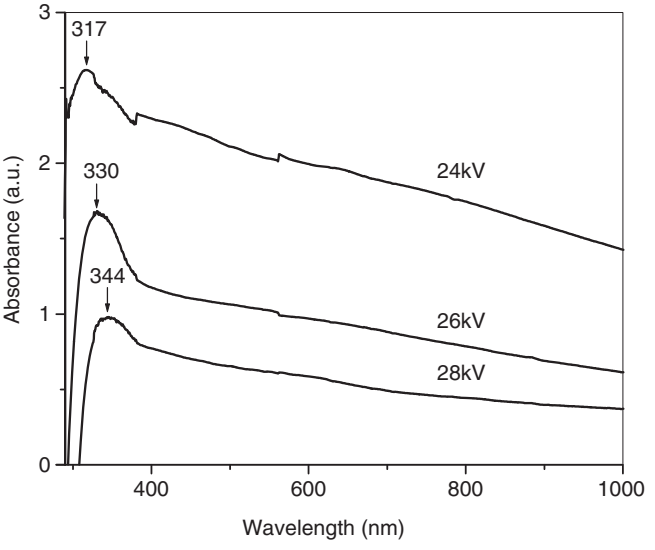

Figure 6. Optical absorption spectra of different laser power-ablated Zn–ZnO nanostructures.

carriers donated by impurities (blue shift of optical band-to-band transitions) lead to Burstein–Moss (BM) effect [24]. The laser ablation of Zn film by lowering laser power creates nanocrystalline or amorphous phase of ZnO [25]. This amorphous phase of ZnO is responsible for a blue shift in absorption spectra. Therefore, the transitional absorption peak, appeared from fabricated Zn–ZnO nanostructure by consecutive lowering the power of laser ablation, might be attributed to exciton absorption from nanocrystalline or amorphous phase of ZnO shell and core metal interband absorption coupling. It is noted that compared to the usual absorption spectrum of ZnO [26,27], the absorption in the visible region of Zn–ZnO system seems to be strong. Generally, ZnO is transparent in the near infrared (NIR) and visible regions but an absorber in the UV region. During pulsed laser irradiation, creation of native defects (mobile point defects) arises in the crystal lattice due to faster nucleation and growth of Zn coated ZnO nanostructure. The strong background below the peak should be due to the strong scattering (Zn nanoparticles are well approximated by spherical) of particles as their sizes are comparable to the light wavelength. The absorption spectra exhibit that the aggregation of nanocrystallites induces more effective photon capturing in the visible region [28]. The existence of a strong light-scattering effect of highly disordered structure on the generating light localisation is also suggested. From this phenomenon it can be concluded that the strong absorption in the visible region of Zn–ZnO core-shell nanostructure could enhance the light harvesting ability and the photocatalysis efficiency. We have observed two pronounced rises (opposite of dips) located in 378 and 560 nm in the optical absorption spectra of Zn–ZnO nanostructure (when the laser ablation was carried out at 24 kV). This type of absorption spectra arises due to Rayleigh–Wood anomaly [29] (related to higher order diffracted waves). Since higher order diffracted waves propagate at a grazing angle to the surface of the grating, they may efficiently couple to surface modes. The core-shell structures fabricated by the laser ablated method have some defects (structural disorder) at the Zn and ZnO interface of core-shell structures and create nanocrystalline or amorphous phase

of ZnO [25]. Therefore, because of overall energy conservation, the diffracted wave along the surface can couple to surface modes of Zn–ZnO nanostructure. This coupling will cause an intensification of the absorbance intensity.

4. Conclusions

The core-shell Zn–ZnO nanostructures were prepared from carbon encapsulated Zn-powder in the thin-film form by laser ablation in the air atmosphere. The structures fabricated by this method show a very strong UV emission at 388 nm. This emission occurs due to free exciton transition through exciton–exciton collision process. Also, very weak blue (486 nm) and green (530 nm) emission peaks originate from defect states. It is also observed that on decreasing laser power, the blue shift of absorption shoulder occurs due to coupling between exciton absorption (from shell layer of nanocrystalline/amorphous ZnO) and core metallic Zn interband absorption. Thus our studies of laser ablated core-shell Zn–ZnO nanostructures using GIXRD, HRTEM, PL (UV-Visible emission) and transitional absorption provide new insights on structural and optical characterisation of Zn–ZnO nanostructures and possible applications for opto-electronic and nanophotonic devices.

Acknowledgements

The authors are grateful to Dr P.K. Datta for providing the laser ablation facility in his laboratory. A. Ghosh acknowledges CSIR, New Delhi, (India) for financial support to carry out this work.

References

[1] P.X. Gao, C.S. Lao, Y. Ding, and Z.L. Wang, *Metal/semiconductor core/shell nanodisks and nanotubes*, Adv. Funct. Mater. 16 (2006), pp. 53–62.
[2] F. Ren, L.P. Guo, Y. Shi, D.L. Chen, Z.Y. Wu, and C.Z. Jiang, *Formation of Zn-ZnO core-shell nanoclusters by Zn/F sequential ion implantation*, J. Phys. D: Appl. Phys. 39 (2006), pp. 488–491.
[3] H. Zeng, W. Cai, J. Hu, G. Duan, P. Liu, and Y. Li, *Violet photoluminescence from shell layer of Zn/ZnO core-shell nanoparticles induced by laser ablation*, Appl. Phys. Lett. 88 (2006), p. 171910(1–3).
[4] J.Q. Hu, Q. Li, X.M. Meng, C.S. Lee, and S.T. Lee, *Thermal reduction route to the fabrication of coaxial Zn/ZnO nanocables and ZnO nanotubes*, Chem. Mater. 15 (2003), pp. 305–308.
[5] X.Y. Zhang, J.Y. Dai, C.H. Lam, H.T. Wang, P.A. Webley, Q. Li, and H.C. Ong, *Zinc/ZnO core-shell hexagonal nanodisk dendrites and their photoluminescence*, Acta Mater. 55 (2007), pp. 5039–5044.
[6] E.M. Wong and P.C. Searson, *ZnO quantum particle thin films fabricated by electrophoretic deposition*, Appl. Phys. Lett. 74 (1999), p. 2939(1–3).
[7] K. Vanheusden, W.L. Warren, C.H. Seager, D.R. Tallant, J.A. Voigt, and B.E. Gnade, *Mechanisms behind green photoluminescence in ZnO phosphor powders*, J. Appl. Phys. 79 (1996), pp. 7983–7990.
[8] J.J. Wu and S.C. Liu, *Low-temperature growth of well-aligned ZnO nanorods by chemical vapor deposition*, Adv. Mater. (Weinheim, Germany) 14 (2002), pp. 215–218.
[9] Q.P. Wang, D.H. Zhang, Z.Y. Xue, and X.T. Hao, *Violet luminescence emitted from ZnO films deposited on Si substrate by rf magnetron sputtering*, Appl. Surf. Sci. 201 (2002), pp. 123–128.

[10] A.F. Kohan, G. Ceder, D. Morgan, and C.G. Van de Walle, *First-principles study of native point defects in ZnO*, Phys. Rev. B 61 (2000), pp. 15019–15027.
[11] S.B. Zhang, S.H. Wei, and A. Zunger, *Intrinsic n-type versus p-type doping asymmetry and the defect physics of ZnO*, Phys. Rev. B 63 (2001), p. 075205(1–7).
[12] F. Mafune, J.Y. Kohno, Y. Takeda, T. Kondow, and H. Sawabe, *Formation of gold nanoparticles by laser ablation in aqueous solution of surfactant*, J. Phys. Chem. B 105 (2001), pp. 5114–5120.
[13] H.B. Zeng, W.P. Cai, B.Q. Cao, J.L. Hu, Y. Li, and P.S. Liu, *Surface optical phonon Raman scattering in Zn/ZnO core-shell structured nanoparticles*, Appl. Phys. Lett. 88 (2006), p. 181905(1–3).
[14] L. Yang, P.W. May, L. Yin, and T.B. Scott, *Growth of self-assembled ZnO nanoleaf from aqueous solution by pulsed laser ablation*, Nanotechnology 18 (2007), p. 215602(1–5).
[15] W. Krätschmer, L.D. Lamb, K. Fostiropoulos, and D.R. Huffman, *Solid C_{60}: a new form of carbon*, Nature 347 (1990), pp. 354–358.
[16] Y. Chen, D.M. Bagnall, H.J. Koh, K.T. Park, K. Hiraga, Z. Zhu, and T. Yao, *Plasma assisted molecular beam epitaxy of ZnO on c-plane sapphire: Growth and characterization*, J. Appl. Phys. 84 (1998), pp. 3912–3918.
[17] D.M. Bagnall, Y. Chen, Z. Zhu, T. Tao, S. Koyama, M.T. Shen, and T. Goto, *Optically pumped lasing of ZnO at room temperature*, Appl. Phys. Lett. 70 (1997), p. 2230(1–3).
[18] P.S. Xu, Y.M. Sun, C.S. Shi, F.Q. Xu, H.B. Pan, *The electronic structure and spectral properties of ZnO and its defects*, Nuclear Instruments and Methods in Phys. Res. B 199 (2003) pp. 286–290.
[19] K. Vanheusden, C.H. Seager, W.L. Warren, D.R. Tallant, and J.A. Voigt, *Correlation between photoluminescence and oxygen vacancies in ZnO phosphors*, Appl. Phys. Lett. 68 (1996), pp. 403–(1–3).
[20] B. Lin, Z. Fu, and Y. Jia, *Green luminescent center in undoped zinc oxide films deposited on silicon substrate*, Appl. Phys. Lett. 79 (2001), p. 943(1–3).
[21] X.Q. Wei, B.Y. Man, M. Liu, C.S. Xue, H.Z. Zhuang, and C. Yang, *Blue luminescent centers and microstructural evaluation by XPS and Raman in ZnO thin films annealed in vacuum, N_2 and O_2*, Physica B 388 (2007), pp. 145–152.
[22] H. Zeng, W. Cai, Y. Li, J. Hu, and P. Liu, *Composition/structural evolution and optical properties of ZnO/Zn nanoparticles by laser ablation in liquid media*, J. Phys. Chem. B 109 (2005), pp. 18260–18266.
[23] H. Amekura, N. Umeda, Y. Sakuma, O.A. Plaksin, Y. Takeda, N. Kishimoto, and C. Buchal, *Zn and ZnO nanoparticles fabricated by ion implantation combined with thermal oxidation, and the defect-free luminescence*, Appl. Phys. Lett. 88 (2006), p. 153119(1–3).
[24] B.E. Sernelius, K.-F. Berggren, Z.-C. Jin, I. Hamberg, and C.G. Graqvist, *Band-gap tailoring of ZnO by means of heavy Al doping*, Phys. Rev. B 37 (1988), pp. 10244–10248.
[25] S.T. Tan, B.J. Chen, X.W. Sun, W.J. Fan, H.S. Kwok, X.H. Zhang, and S.J. Chua, *Blueshift of optical band gap in ZnO thin films grown by metal-organic chemical-vapor deposition*, J. Appl. Phys. 98 (2005), p. 013505(1–5).
[26] H. Yoshikawa and S. Adachi, *Optical Constants of ZnO*, Jpn. J. Appl. Phys. 36 (1997), pp. 6237–6243.
[27] L. Bergström, A. Meurk, H. Arwin, and D.J. Rowcliffe, *Estimation of hamaker constants of ceramic materials from optical data using lifshitz theory*, J. Am. Ceram. Soc. 79 (1996), pp. 339–348.
[28] Q. Zhang, T.P. Chou, B. Russo, S.A. Jenekhe, and G. Cao, *Aggregation of ZnO nanocrystallites for high conversion efficiency in dye-sensitized solar cells*, Angew. Chem. Int. Ed. 47 (2008), pp. 2402–2406.
[29] E.W. Palmer, M.C. Hutley, A. Franks, J.F. Verrill, and B. Gale, *Diffraction gratings*, Rep. Prog. Phys. 38 (1975), pp. 975–1048.